Journal of the Algerian Chemical Society

Journal homepage : https://www.jacs-dz.org

ISSN 1111-4797

Volume 34, Issue 1
January 2024

STRUCTURAL AND PHOTOLUMINESCENCE PROPERTIES OF EU^{3+} DOPED $(GD_{1-X}LU_X)_3AL_5O_{12}$ SYNTHESIZED BY SOLID STATE REACTION

Imane Lanez, Brahim, Rekik, Nesrine Naimi

LPCMIA Laboratory, Department of Physics, Faculty of Sciences, Saad Dahleb Blida 1 University, Blida, BP 270 Soumaa Road Blida, Algeria

Article History

Received: 13/05/2024

Revised: 11/11/2024

Accepted: 12/11/2024

ABSTRACT

The $(Gd_{1-x}Lu_x)_3Al_5O_{12}$ garnet compounds doped with 5% Eu^{3+} were synthesized using the solid-state reaction method calcined at 1450°C. Despite the stabilization of the phase $Gd_3Al_5O_{12}$ by lutetium and doped europium, XRD structural analysis revealed the presence of secondary phases, including sesquioxide (R: Ln_2O_3), monoclinic garnet (M: $Ln_4Al_2O_9$), and perovskite (P: $LnAlO_3$) as major phase, accompanied the cubic garnet (G: $Ln_3Al_5O_{12}$) phase. FTIR results confirmed the structure of the samples identified the characteristic bands of all observed phases. The energy transfers of Gd^{3+} enhance the luminescence of Eu^{3+}activator ions. Photoluminescence analysis indicated that Eu^{3+} improves structural symmetry within the luminescent host materials. Under excitation at 360 nm, the non-centrosymmetric phases R, M and P were identified by the dominance of electric dipole $^5D_0$ to $^7F_2$ transitions. In contrast, the emission from centrosymmetric cubic garnet doped with Eu^{3+} presents by the magnetic dipole $^5D_0$ to $^7F_1$ dominant transition.

Keywords: Europium, solid state reaction, XRD, FTIR, photoluminescence.

1. INTRODUCTION

Cubic garnet compounds attract significant attention due to their excellent chemical and structural stability and optical isotropy for a variety of applications [1]. The best example of a garnet compound is $Y_3Al_5O_{12}$ doped with rare earth elements, which crystallizes in the cubic structure with the Ia-3d space group and has a general formula of $Ln_3Al_5O_{12}$ (LnAG: Y and lanthanide). In this structure, Ln atoms occupy the dodecahedral coordination 24 (c) sites, Al atoms occupy the octahedral 16 (a) and tetrahedral 24 (d) sites, and O atoms occupy the 96 (h) sites. Because of their good optical properties, multi compounds cubic garnet materials $(Gd, Lu)_3Al_5O_{12}$ doped with europium are highly competitive in fluorescence fields [2]. Stable cubic garnet structures are found in elements ranging from lutetium (Lu^{3+}) to terbium (Tb^{3+}), but not for ions larger than Gd^{3+} [3]. Solid state reactions between Ln_2O_3 and Al_2O_3 metal oxides can produce LnAG powder compounds. However, these reactions often result in the formation of secondary phases such as monoclinic garnet $Ln_4Al_2O_9$ and perovskite $LnAlO_3$, which require significantly higher temperature to eliminate [4]. Our objective is to distinguish the different structural phase transformations by the occupation of europium in sesquioxides, monoclinic garnet, perovskite and cubic garnet intermediate phases that appear in the Eu^{3+} doped $(Gd_{1-x}Lu_x)_3Al_5O_{12}$ samples elaborated by solid state reaction method and calcined at T=1450°C. The vibrational characterizations were used to determine the different bands associated to the various frequencies of these phases (R, M, P and G). The luminescent properties of Eu^{3+} doped $(Gd_{1-x}Lu_x)_3Al_5O_{12}$ with (x=0.2 and 0.3) are discussed in this paper through europium transitions to evaluate Ln_2O_3, $Ln_4Al_2O_9$, $LnAlO_3$, and $Ln_3Al_5O_{12}$ phase formation in our samples. The intrinsic $^8S_7 \rightarrow {}^6I_J$ transition of Gd^{3+} can be achieved via an efficient energy transfer from Gd^{3+} to the activator doping element Eu^{3+} [5], which occupied D2 point symmetry in the cubic garnet centrosymmetric structure [6], [7]. The emission in these materials is presented by the main peak corresponding to the $^5D_0 \rightarrow {}^7F_1$ dominant transition, due to the magnetic dipolar [3]. However, the sesquioxide, monoclinic garnet, and perovskite were regarded as Eu^{3+} doped matrix materials [3] [8]. These types of materials lack inversion symmetry (non-centrosymmetric) [3], corresponding to the dominant $^5D_0 \rightarrow {}^7F_2$ transitions due to the electric dipole in each phase (R, M, and P).

2. RESULTS AND DISCUSSION

2.1. XRD structural study

XRD analysis were affected to observe the different effects on the structural properties of $(Gd_{1-x}Lu_x)_3Al_5O_{12}$ with x=0.2 and 0.3 calcined at T=1450°C, especially the effect of calcinations temperature on the formation of garnet phase.

2.1.1. The effect of temperature

Calcination temperature influences phase formation through the polymorphic changes of the Gd_2O_3, Lu_2O_3 and Al_2O_3 as raw materials to form $(Gd_{1-x}Lu_x)_3Al_5O_{12}$ synthesized by the solid state reaction method, calcined at T=1450°C.

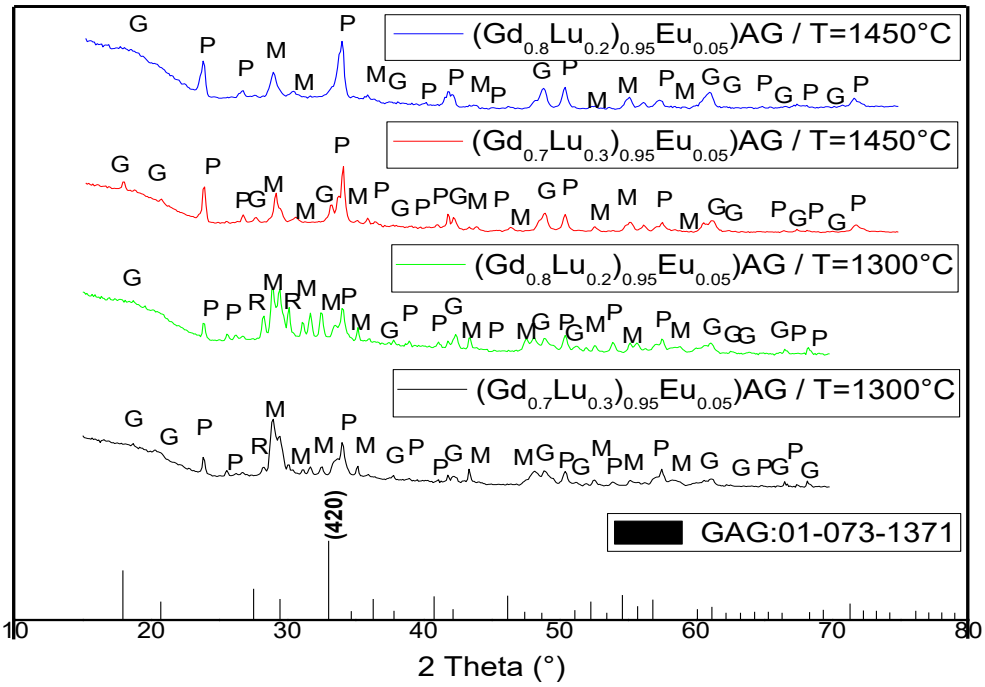

Fig.1. XRD pattern of 5at% Eu^{3+} doped $(Gd_{0.7}Lu_{0.3})_3Al_5O_{12}$ and $(Gd_{0.8}Lu_{0.2})_3Al_5O_{12}$ samples calcined at T= 1300°C and 1450°C, with R, M, P, and G representing Ln_2O_3 sesquioxides, LnAM monoclinic garnet, LnAP perovskite, and LnAG garnet, respectively, and Ln = Gd, Lu

The evolution of Ln_2O_3 sesquioxide phases follows the structure of $Ln_4Al_2O_9$ monoclinic garnet, $LnAlO_3$ perovskite phases, and $Ln_3Al_5O_{12}$ cubic garnet phases as a function of synthesis temperature [5]. The reactions are as follows [2]:

(R) (M) (P) (G)

$$\mathbf{Ln_2O_3 \longrightarrow Ln_4Al_2O_9 \longrightarrow LnAlO_3 \longrightarrow Ln_3Al_5O_{12}}$$

$Lu_3Al_5O_{12}$ cubic garnet is known as a very stable phase because it contains tiny Lu^{3+}cations at sites with coordination number 8 and point symmetry D2 without decompositions [2,3], and it crystallizes in the space group Ia-3d. Garnet $Gd_3Al_5O_{12}$ is a metastable phase, but it can be stabilized with Lu^{3+} and GdLuAG with larger ions than Gd^{3+}, such as Eu^{3+} (r= 1.066 A°) [7]. Fig.1 depicts the XRD pattern of the $(Gd_{1-x}Lu_x)_3$ Al_5O_{12}:Eu^{3+} with x= 0.2 and 0.3 samples calcined at T=1300°C and 1450°C respectively. For the samples $(Gd_{1-x}Lu_x)_3$ Al_5O_{12}:Eu^{3+} with x= 0.2 and 0.3 calcined at 1300°C, we observed the elimination and decrease of certain peaks associated with the monoclinic garnet in the Eu^{3+} doped $(Gd_{0.7}Lu_{0.3})_3$ Al_5O_{12} samples compared to $(Gd_{0.8}Lu_{0.2})_3$ Al_5O_{12}. Additionally, for the powders $(Gd_{1-x}Lu_x)_3$ Al_5O_{12}:Eu^{3+} with x= 0.2 and 0.3 calcined at 1450°C, we observed the appearance of the main peak (420) of cubic garnet in the $(Gd_{0.7}Lu_{0.3})_3$ Al_5O_{12} sample compared to $(Gd_{0.8}Lu_{0.2})_3$ Al_5O_{12} doped with europium. This is due to the increased lutetium concentration, which is considered a stabilizer of GAG. Furthermore, as the calcination temperature rises from 1300 to 1450°C, the cubic garnet is formed. The major phase formed in all samples is the gadolinium perovskite phase ($GdAlO_3$), which forms due to the larger ionic radius of gadolinium (r Gd =1.053A°) compared to lutetium (r Lu= 0.977A°). As a result, Gd^{3+} alone does not form GAG cubic garnet, but it can easily form the structure of perovskite, as shown in the phase diagram of the binary system Gd_2O_3-Al_2O_3 [2]. The choice of these solid solutions Eu^{3+} doped $(Gd_{1-x}Lu_x)_3Al_5O_{12}$ for x= 0.2 and 0.3 was based on phase stability as well as improved optical performance, as detailed in [3]. The effect of the ionic size of the substituent element lutetium, which has a radius (0.977A°) less than that of gadolinium (1.053A°), on the coordination 8 [6], [3]. $GdAlO_3$ (GAP) is the main phase crystallized in an orthorhombic structure with the space group Pbnm perovskite structure, and the majority of diffraction peaks are indexed using PDF card no. 46-0395 [3]. The lattice parameters calculated by High Score software for the sample $[(Gd_{0.8}Lu_{0.2})_{0.95}Eu_{0.05}]_3Al_5O_{12}$ from the XRD spectrum shown in fig 1 are a = 5.310375 A°, b = 7.435087 A°, and c = 5.2454469 A°, which are higher than those of $(Gd_{0.8}Lu_{0.2})_3Al_5O_{12}$, and the different cell parameters for the sample $[(Gd_{0.7}Lu_{0.3})_{0.95}Eu_{0.05}]_3Al_5O_{12}$ are a = 5.310375 A°, b = 7.43029 A°, and c =5.236558 A°. The decrease in the values of the lattice parameters b and c due to the lutetium content (x=0.2 and 0.3) and the calcination temperature. The observed perovskite phases decrease due to the 3:5 synthesis starting stoichiometry (Ln_2O_3/Al_2O_3), while the calcination temperature increases to form cubic garnet phases $Ln_3Al_5O_{12}$. The structure of [(Gd_{1-}

$_xLu_x)_{0.95}Eu_{0.05}]]_3Al_5O_{12}$ crystallizes in a cubic system with space group O_h^{10} Ia-3d and lattice parameters around 12.00 A°, which is close to the ionic radius of $Tb_3Al_5O_{12}$ [2], [9]. (GdAG, JCPDS file No. 1-73-1371). It is clear that the content of Gd, which reduces the average ionic size of rare earth ions to 1.0454 A° [10], is directly related to garnet formation. Because thermodynamically stable LnAG only exists for Ln^{3+} smaller than Gd^{3+}, which serves as the boundary element for the formation of the garnet structure [10], it can effectively stabilize GdAG. The Al_2O_3 diffraction peaks were also missing in the two samples (x =0.2 and 0.3). Unreacted Al_2O_3 should be present in the calcined products of these samples up to 1450°C for the initial stoichiometry in systems prepared using the solid-state reaction method [6]. However, at higher temperatures (T >1500 °C), the remaining Al_2O_3 reacts with GAP to form pure GAG garnet [2], [10].

2.2. Vibrational characterizations by FTIR

FTIR spectra were established using the samples $(Gd_{1-x}Lu_x)_3Al_5O_{12}$ (x= 0.2 and 0.3) to investigate the functional groups presented by active vibrations modes in IR. In this step, we will examine the vibrational properties of the samples as they change with temperature. Fig.2 and 3 show the FTIR spectra for x=0.2 and 0.3 were calcined at T=1300°C and T=1450°C, respectively. Due to the low synthesis temperature, the studied systems are always multi-phases: R, M, P, and G. Fig. 3, 4, and 5 show the bond vibrations between M-O, where M represents Gd, Lu, or Al, in all phases that appear. Fig. 4 depicts the undoped and doped $[(Gd_{1-x}Lu_x)_{0.95}Eu_{0.05}]_3Al_5O_{12}$ compounds with x=0.2 and 0.3 with 5% Eu^{3+}. The characteristics M-O vibrations are associated with specific peaks in the 400-1000 cm^{-1} region of the IR spectra (M: Gd, Lu, Al). The vibrations of isolated $[AlO_4]$ and $[AlO_6]$ at 795 and 730 cm^{-1} in tetrahedral and octahedral sites, respectively, and 743.6 cm^{-1} indicate the formation of the (Gd, Lu-O) bonds of $(Gd, Lu)_3Al_5O_{12}$ phases [11] [12], [13]. The vibration modes of Gd-O in $GdAlO_3$ [14] [15], [16], [17], and [18] correspond to the peaks at 417,420, and 519 cm^{-1}, as well as the peaks at 460,470, and 651,655, and 664, 669 cm^{-1}, which appeared due to the Al-O stretching band characteristic vibration in $GdAlO_3$[19], [20]. The Al-O vibrations of $Ln_4Al_2O_9$ have peaks at 792 and 681,684 and 686 cm^{-1}, whereas the Ln-O vibrations have peaks at 718 and453, 457 cm^{-1} [21]. The absorption bands in the range of 477 and 582 cm^{-1} can be attributed to Lu-O stretching modes in Lu_2O_3 [22], [24], [5], and the peaks around 438,448, and 540 cm^{-1} can be attributed to bond Gd-O stretching and bending vibrations in Gd_2O_3 [20] [21] [22].

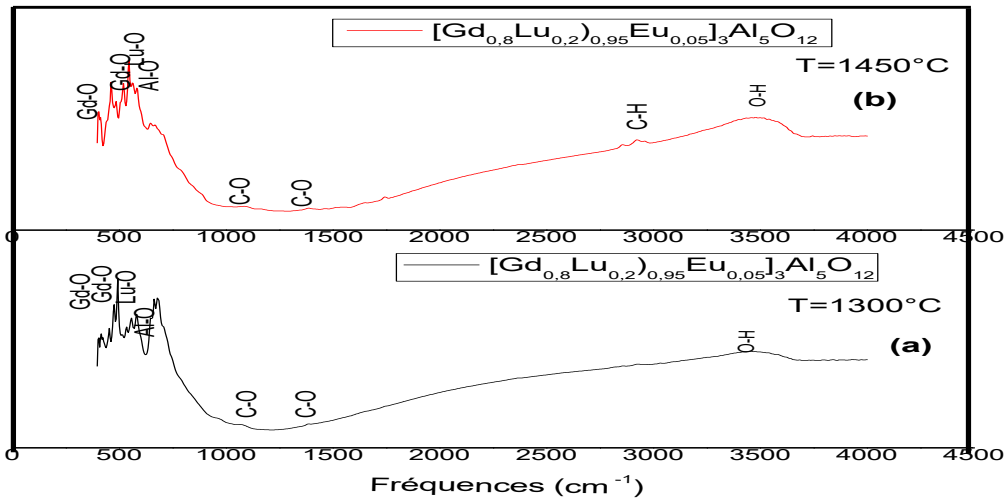

Fig.2. FTIR spectra of 5 at% Eu^{3+} doped $(Gd_{0.8}Lu_{0.2})_3Al_5O_{12}$ calcined at (a): T=1300°C and (b) T=1450°C

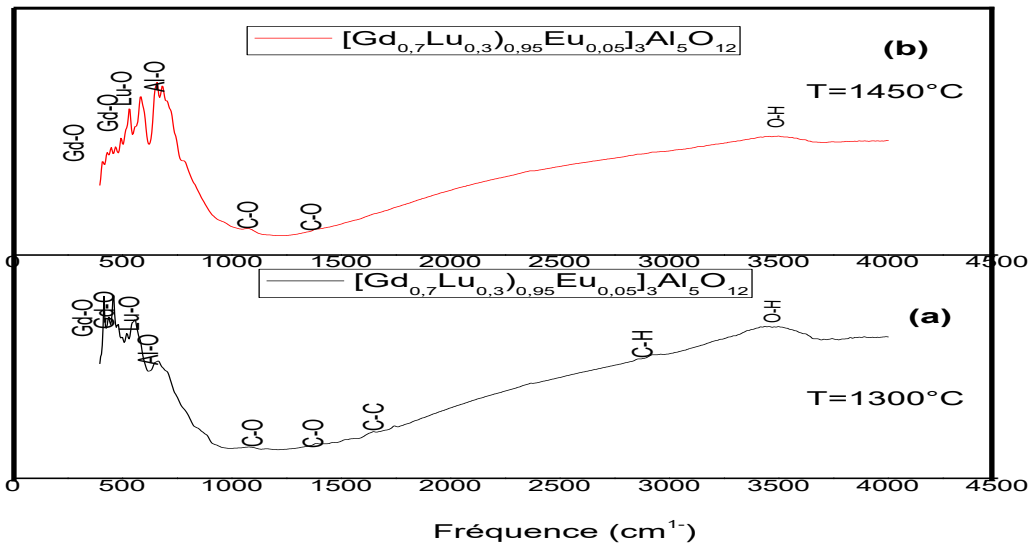

Fig.3. FTIR spectra of 5% Eu^{3+} doped $(Gd_{0.7}Lu_{0.3})_3Al_5O_{12}$ with calcined at (a) T= 1300°C and (b) T=1450°C

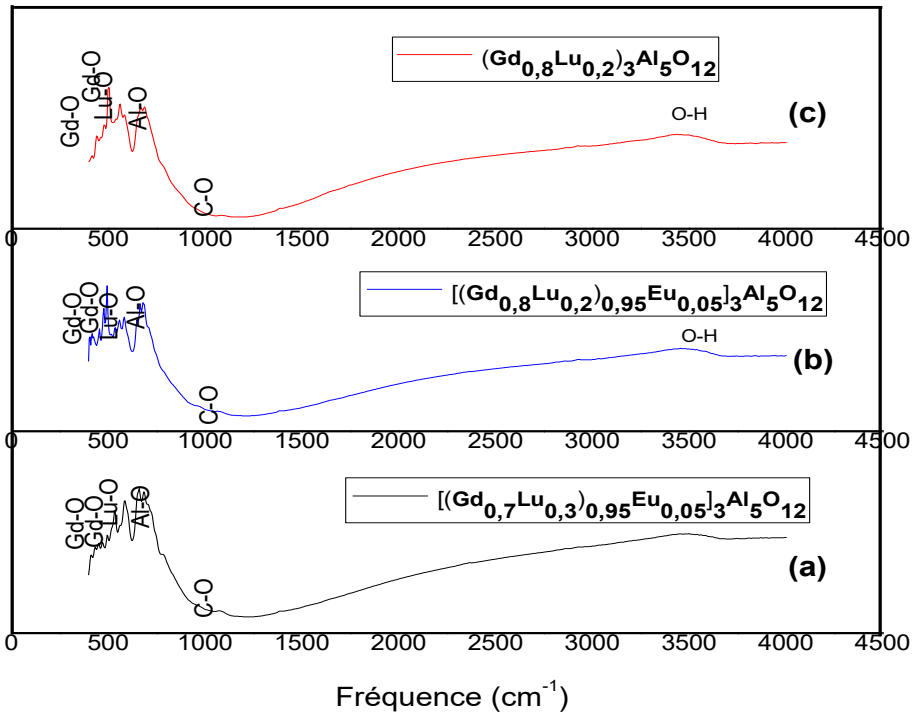

Fig.4. FTIR spectra of undoped and 5 at% Eu^{3+} doped $(Gd_{0.8}Lu_{0.2})_3Al_5O_{12}$ and $(Gd_{0.7}Lu_{0.3})_3Al_5O_{12}$ calcined at T = 1450°C

Other external absorption peaks near 3000-3710 cm^{-1} are due to H_2O stretching [20]. Peaks at 3467,3495 cm^{-1} [2] and 1643 [7] cm^{-1} provide evidence of water hydration in the structure or surface adsorbed water, and are assigned to the O-H stretching and H-O-H bending modes, respectively. The bands at 3500-3750 cm^{-1} correspond to hydroxyl (OH) groups [12], the band at 1070 cm^{-1} corresponds to the C-O symmetric stretching vibration [12], and the bands at 1518 and 1393 cm^{-1} correspond to the C-O asymmetrical stretching vibrations. The C=C-links in the synthesized compound are represented by the peak at 1564 cm^{-1}, which is due to atmospheric carbon absorption, and the peaks at 1175-1385 cm^{-1} and 1600-1700 cm^{-1} are due to stretching-CO-OH group vibrations [7], [12]. Absorption peaks of gadolinium garnet from undoped and Eu^{3+}doped $(Gd_{1-x}Lu_x)_3Al_5O_{12}$ with x=0.2 and 0.3 [23], [2] were observed at 600 cm^{-1} from M-O vibration. This result is similar to the XRD patterns.

2.3. Photoluminescence

The emission spectra of the samples $[(Gd_{1-x}Lu_x)_{0.95}Eu_{0.05})]_3Al_5O_{12}$ with x=0.2 and 0.3 calcined at T=1450°C, studied in the visible spectral domain under an excitation of 360 nm for europium doping are shown in fig.5 and 6 respectively. Due to the presence of europium transitions as an activator

element and the stark splitting of these compounds [8], all PL spectra of the elaborated samples show the same types of europium transitions. Due to the lower electronegativity in the systems $(Gd_{1-x}Lu_x)_3Al_5O_{12}$[2] doped with rare earth [3], the attribution of Gd^{3+} exhibits higher lattice covalence and charge transfer, which enhances crystal field splitting of high energy level of Eu^{3+} (5d). Reference [5] compared the electronegativity of the systems: $(Gd_{0.8}Lu_{0.2})_3Al_5O_{12}$ and $(Gd_{0.7}Lu_{0.3})_3Al_5O_{12}$ to that of $Ln_3Al_5O_{12}$, where Ln: Lu, Y, and Gd. We observe a proportional evolution between the gadolinium content and the emission intensities of Eu^{3+} in the elaborated samples: Eu^{3+}doped $(Gd_{1-x}Lu_x)_3Al_5O_{12}$, due to the energy transfer from ggadolinium to the europium activator element [3]. The optimum of Eu^{3+} concentration is estimated to be 5at% [3]. It should also be noted that a small shift in position and wavelength values in the samples $[(Gd_{0.8}Lu_{0.2})_{0.95}Eu_{0.05}]_3Al_5O_{12}$ and $[(Gd_{0.7}Lu_{0.3})_{0.95}Eu_{0.05})]_3\ Al_5O_{12}]$ may be due to the amount of gadolinium substituted with lutetium in the solid solution which x = 0.2 and 0.3 and effect of calcination temperature [2]. Figures 5 and 6 present a stronger emission in the visible spectral domain. The $^5D_0 \rightarrow {}^7F_0$ transition of Eu^{3+}, which occurs around (580 nm), is only allowed for low symmetry sites or materials that do not have an inversion center [2], [3]. The large intensity of the $^5D_0 \rightarrow {}^7F_3$ and $^5D_0 \rightarrow {}^7F_4$ transitions around 700 nm may be due to the presence of mixtes phases [8], [3]. We can divide this range into two regions because there are two types of broad peaks centered at a wavelength range (from 580 to 640 nm). In the first region, Eu^{3+} binds to non-centrosymmetric sites of the symmetry points m-3, C1, or Cs, which correspond to the cubic bixbyite sesquioxides Ln_2O_3 with space group Ia-3, the monoclinic garnet structure of $Ln_4Al_2O_9$ with space group P21/c, and the orthorhombic perovskite structure of $LnAlO_3$ phases with space group Cs, respectively. This is similar to the case of 2 at% Eu^{3+} doped $LiGd(WO_4)_2$ powders and crystals fibers, which present Eu^{3+} transitions observed in others tungstate hosts with the dominance of $^5D_0 \rightarrow {}^7F_2$ transition in the emission spectrum, confirming the presence of low symmetry site of Eu^{3+} located in these types of materials [25].

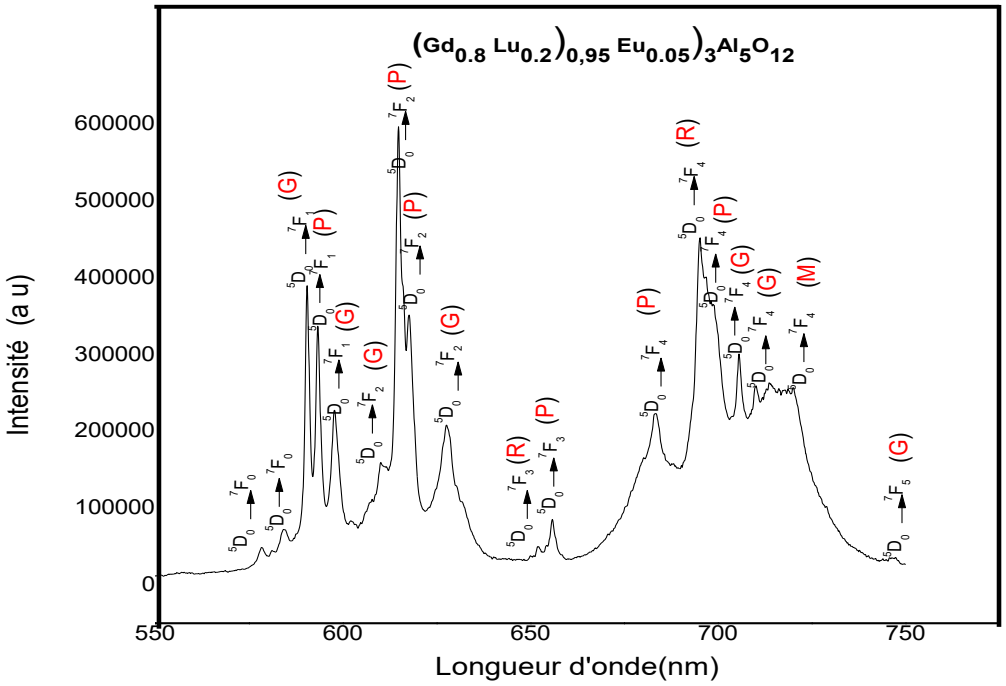

Fig.5. PL spectrum of $[(Gd_{0.8}Lu_{0.2})_{0.95}Eu_{0.05}]_3 Al_5O_{12}$ calcined at 1450°C

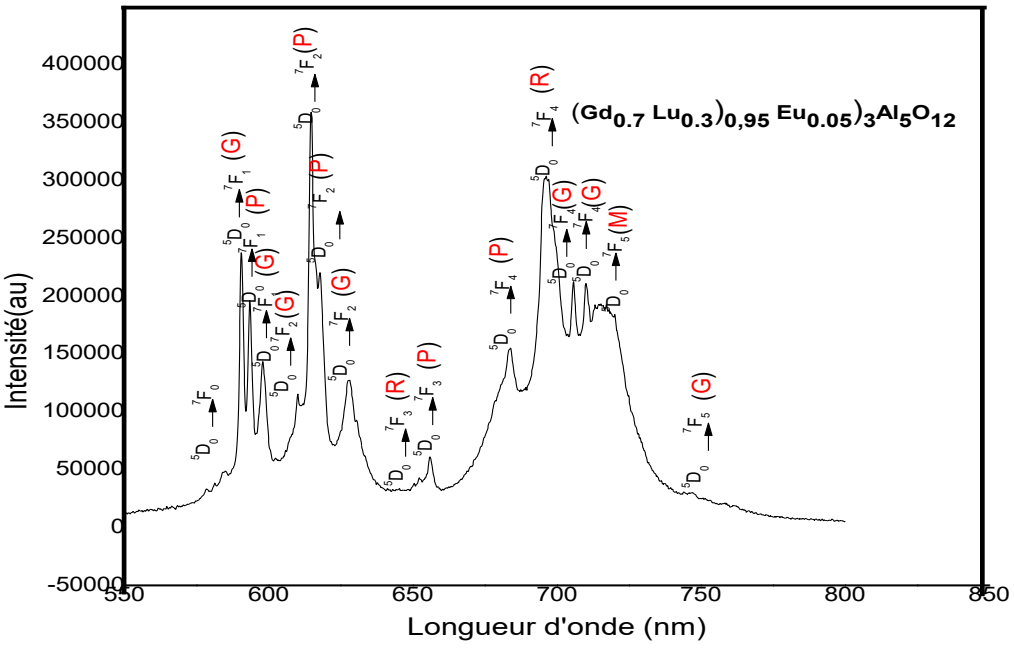

Fig.6. PL spectrum of $[(Gd_{0.7}Lu_{0.3})_{0.95}Eu_{0.05}]_3Al_5O_{12}$ calcined at 1450°C

As a result, the electric dipole (ED) $^5D_0 \rightarrow {}^7F_2$ emissions are stronger than the magnetic dipole (MD) $^5D_0 \rightarrow {}^7F_1$ emissions. In the second region, corresponding to the centrosymmetric sites occupied by europium, we find cubic garnet materials with space group Ia-3d and point D_2 symmetry of $Ln_3Al_5O_{12}$ phases. Consequently, the PL spectra are dominated by the $^5D_0 \rightarrow {}^7F_1$ magnetic dipole transition rather than the $^5D_0 \rightarrow {}^7F_2$ electric dipole transition. The different transitions of Eu^{3+} in the phases that appeared and the symmetry or asymmetry factors that represent the ratio of the intensities of the peaks correspond to non-centrosymmetric positions occupied by Eu^{3+} transitions of electric and magnetic dipoles respectively. For the sesquioxide in the systems elaborated $[(Gd_{0.8}Lu_{0.2})_{0.95}Eu_{0.05})]_3Al_5O_{12,}$ and $[(Gd_{0.7}Lu_{0.3})_{0.95}Eu_{0.05})]_3\ Al_5O_{12}$ calcined in the T=1450°C, the asymmetry factors related to the ratio $I_{611}/\ I_{585}$[3], [26], as well as the asymmetry factors for the monoclinic LnAM phases are 0.881 and 0.354 in these two elaborated samples, which are presented by the transition I_{606} / I_{592} [3], [21]. These phases are considered secondary phases to achieve the formation of perovskite and pure cubic garnet phases. It is worth noting that this asymmetry factor increases as a function of Gd^{3+} content for the Ln_2O_3 sesquioxide and $Ln_4Al_2O_9$ monoclinic phases, indicating that it has the benefit of charge transfer to the activator element Eu^{3+} [3], [7]. More optical findings necessitate an increase in gadolinium content, but with the ideal choice of Eu^{3+} (5at %) as the optimum concentration to prevent the quenching. The monoclinic garnet phase has received less attention in the literature than the other phases, P, and G [27]. On the other hand, perovskite phases are the majority phases in the elaborated compounds $[(Gd_{0.8}Lu_{0.2})_{0.95}Eu_{0.05})]_3Al_5O_{12}$ and $[(Gd_{0.7}Lu_{0.3})_{0.95}Eu_{0.05})]_3\ Al_5O_{12}$. The asymmetry factors in these elaborated samples are 2.239 and 2.526, respectively, as illustrated by I_{614} / I_{593} transitions [28], [29]. These values were compared with the value ~ 2.16 in the reference [3], and the increase of the factor may be due to the addition of lutetium, which has a smaller ionic radius and is less likely to form a perovskite phase. The phase diagrams Gd_2O_3-Al_2O_3 and Eu_2O_3-Al_2O_3 indicate that due to the larger ionic radius of Gd^{3+} and Eu^{3+}, the synthesis of the perovskite phases $GdAlO_3$ and $EuAlO_3$ is easier. In contrast, lutetium, with it's a smaller ionic radius, makes the formation of the $LuAlO_3$ perovskite phase difficult, and it is considered a metastable phase. This is similar to the behaviour of gadolinium in the formation of $Gd_3Al_5O_{12}$ cubic garnet materials [2]. However, the ionic size compensations between the ions Gd^{3+}, Lu^{3+}, and Eu^{3+} under the influence of calcination temperature increased the value of the asymmetry factor between the $[(Gd_{0.8}Lu_{0.2})_{0.95}Eu_{0.05})]_3Al_5O_{12}$ and $[(Gd_{0.7}Lu_{0.3})_{0.95}\ Eu_{0.05})]_3Al_5O_{12}$ samples with x=0.2 and 0.3. Additionally, as this component increased, the concept of charge transfer from Gd^{3+}

to Eu^{3+} in perovskite phases and cubic garnets existed [3], which occurred during the formation and polymorphic transitions from perovskite phases to cubic garnets phases. The symmetry factors determined from the photoluminescence spectra, associated with the transition I_{591}/ I_{610} [3], [6], [7], [10] for the cubic garnets phases of these powders calcined at T=1450°C, is 1.707 and 1.557 at x= 0.2 and 0.3 respectively. These symmetry factors decrease as the ggadolinium content decreases. The symmetry factor for the garnet phases [7],[30] is close to one, implying that Eu^{3+} ions occupy the same ratio of symmetry and asymmetry sites. This approach confirms the transition from perovskite phases to cubic garnet with an inversion center. The evolution of this phase was already approved by firstly the increasing of llutetium, which is considered a stabilizer of the systems Eu^{3+} doped $(Gd_{0.8}Lu_{0.2})_3Al_5O_{12}$ to $(Gd_{0.7}Lu_{0.3})_3Al_5O_{12}$ [7], and second, by the rising content of lutetium, which is considered a stabilizer of the systems. The ratio of intensity, which shows the site occupied by Eu^{3+} in all structures that appeared R, M, and P during the formation of cubic garnet, was primarily due to the dominance of the magnetic dipole transition. This is attributed to the use of the solid state reaction method, which requires raising the temperature to more than 1500 °C to obtain pure cubic garnet phases [2]. Consequently, the electric dipole transition $^5D_0 \rightarrow ^7F_2$ emission should be suppressed, and only the $^5D_0 \rightarrow ^7F_1$ magnetic transition will be dominant [3]. Moreover, these photoluminescence results of garnet phase are well coherent with $Ln_3Al_5O_{12}$ pure garnets host materials like $Y_3Al_5O_{12}$ and $Lu_3Al_5O_{12}$ doped with Eu^{3+} phosphors respectively [31], [32].

3. EXPERIMENTAL

The solid state reaction method was used to elaborate undoped and 5% Eu^{3+} doped $(Gd_{1-x}Lu_x)_3Al_5O_{12}$ (x=0,2-0,3) polycrystalline powders. The raw materials are: Gd_2O_3 (99.99%), Lu_2O_3 (99.99%), Alfa-Al_2O_3 (99.99%), and Eu_2O_3 (99.99%) were mixed thoroughly in an agate mortar, and calcined at T=1300 and 1450°C with a heating rate of 5 °C/min. for 72 hours. The solid-state process was used to make the samples $[(Gd_{1-x}Lu_x)_{1-y}Eu_y]_3Al_5O_{12}$ with x=0.2 and 0.3 according to the chemical equation:

$$3[(Gd_2O_3(1-x)+xLu_2O_3)]_{1-y}+yEu_2O_3+5Al_2O_3 \rightarrow 2[(Gd_{1-x}Lu_x)1-yEuy]_3Al_5O_{12}$$

The samples were identified by X-ray diffraction (XRD), acquired with a Bragg-Brentano Bruker D_2 Advance diffractometer working with the Cu Ka radiation (=1.54A°), owing to a backward monochromator, after the preparation of powders, undoped and doped with 5% at Eu^{3+}. The

vibrational studies were characterized by infrared spectroscopy as KBr pellets in the 400-4000 cm^{-1} region using a JASCO-4100 FTIR Fourier Transform Spectrometer. The photoluminescence (PL), analysis with excitation by laser for visible luminescence, was performed by an Ekspla NT342 optical parametric oscillator (OPO), with a resolution of 0.2 nm using 1200 lines/mm, and analyzed with an iSTAR CCD.

4. CONCLUSION

In summary, we used the solid state reaction method to elaborate 5 at% Eu^{3+} doped $(Gd_{1-x}Lu_x)_3Al_5O_{12}$ with (x=0.2 and 0.3) at calcination temperatures (T=1300°C and 1450°C). XRD analysis of the structure of compounds reveals the presence of perovskite ($LnAlO_3$) as the major phase in a high proportion (0.7and 0.8) of gadolinium calcined at T= 1450°C, with the remaining phases being Ln_2O_3, $Ln_4Al_2O_9$, and $Ln_3Al_5O_{12}$. The vibrational study by FTIR spectroscopy is an important step for determining the following bands characterizing: Gd-O, Lu-O, and Al-O, as well as the active modes of vibration of the phases appearing at 5 at% Eu^{3+} doped $(Gd_{0.8}Lu_{0.2})_3Al_5O_{12}$ and $(Gd_{0.7}Lu_{0.3})_3Al_5O_{12}$ compounds with external modes such as O-H, C-O, C-C CO-OH... To further validate the influence of Gd^{3+} substitution on Eu^{3+} emission, the studied systems should be an important type of phosphor. The presence of the $^5D_0 \rightarrow {}^7F_J$ transition peaks due to the europium correlating to distinct phases with the major $LnAlO_3$ phases can be seen in the photoluminescence spectra. Through the $^5D_0 \rightarrow {}^7F_2$ and $^5D_0 \rightarrow {}^7F_1$ transitions, which correspond to electric and magnetic transition dipoles respectively, the Eu^{3+} site provides a strong investigation into the crystalline structure and symmetry. The electric dipole $^5D_0 \rightarrow {}^7F_2$ is more intense than the magnetic dipole $^5D_0 \rightarrow {}^7F_1$ in structures without symmetry centers such as R (Ln_2O_3), M ($Ln_4Al_2O_9$), and P($LnAlO_3$), but the magnetic dipole $^5D_0 \rightarrow {}^7F_1$ is a more intense in structures with an inversion point of symmetry such as garnet phase. The luminous symmetry factor for developed samples $[(Gd_{1-x}Lu_x)_{0.95}Eu_{0.05})]_3Al_5O_{12}$, with x=0.2 and 0.3 at T= 1450°C, indicates both a tendency for phase formation and an increase in luminescent intensity for high Gd^{3+} concentration due to energy transfer from it to Eu^{3+} activator.

5. REFERENCES

[1] Marlot, C.; Barraud, E.; Le, S.; Eichhon, M. Synthesis of YAG nanopowder by the co-precipitation method: Influence of pH and study of the reaction mechanisms. *J. Solid State Chem*. **2012,** 191,114-120.

[2] Li, J.; Li, J.G.; Zhang, Z.; Wu, X.; Liu, S.; Li, X., Sun, X.; Sakka, Y. Gadolinium Aluminate Garnet (Gd3Al5O12): Crystal Structure Stabilization via Lutetium Doping and Properties of the (Gd 1− x Lu x) 3 Al5O12 Solid Solutions (x= 0–0.5). *J. Am. Ceram. Soc.* **2012,** 95, 931-936.

[3] Li, J.; Li, J.G.; Li, J.; Liu, S.; Li, X., Sun, X.; Sakka, Y. Development of Eu3+ activated monoclinic, perovskite, and garnet compounds in the Gd2O3–Al2O3 phase diagram as efficient red-emitting phosphors. *J. Solid State Chem*. **2013,** 206,104-112.

[4] Lanez,I.; Rekik,B.; Kezzim,A.; Derbal,M.; Lanez,T.; Lebbou,K. ; Structural and vibrational properties of $(Gd_{0.7}Lu_{0.3})_3Al_5O_{12}$ cubic garnet synthesized with different aluminum sources via co precipitation method. *Bull Material Sci.* **2024,** 47, 31-94.

[5] Lanez, I., Rekik; B.; Derbal, M.; Chaib, A. Structural study and the effect of ionic size of the systems (Gd1-x Lux) 3Al5 O12 doped erbium. *J. Fundam. Appl. Sci.* **2019,** 11, 857-874.

[6] Li, J.; Li, J.G.; Sakka, Y.; Investigation of new red phosphors of Eu^{3+} activated (Gd, Lu) 3Al5O12 Garnet. *Inter. J. Mat. Sci. Eng*. **2013,** 1, 15-19.

[7] Li, J.; Li, J.G.; Zhang, Z.; Wu, X.; Liu, S.; Li, X., Sun, X.; Sakka, Y. Effective lattice stabilization of gadolinium aluminate garnet (GdAG) via Lu^{3+} doping and development of highly efficient (Gd, Lu) AG: Eu^{3+} red phosphors. *Sci. Technol. Adv. Mater.* **2012,**13.

[8] Binnemans, K.; Interpretation of europium (III) spectra. *Coord. Chem. Rev.* **2015,** 295, 1-45.

[9] Li, J.G.; Li, J.; Zhu, Q.; Wang.; Li, X., Sun, X.; Sakka, Y. Photoluminescent and cathodoluminescent performances of Tb 3+ in Lu 3+-stabilized gadolinium aluminate garnet solid-solutions of [(Gd 1− x Lu x) 1− y Tb y] 3 Al 5 O 12. *RSC Advances*. **2015,** 73, 59686-59695.

[10] Li, J.G.; and Sakka, Y.; Recent progress in advanced optical materials based on gadolinium aluminate garnet (Gd3Al5O12). *Sci. Tec. Adv. Mat*. **2015,** 16, 014902.

[11] Papagelis, K.; Ves, S. Vibrational properties of the rare earth aluminum garnets. *J. Appl. Phys.* **2003,** 10, 6491-6498.

[12] Boukerika, A.; Guerbous, L. Effect of Y3+ substitution on structural and photoluminescence properties of solid solutions [(Lu1− xYx) 1− z Cez] 3Al5O12 phosphors. *Mater. Chem. Phys.* **2016,** 394-399.

[13] Praveena, R.; Shim, J.J.; Cai, P.; Seo, H.J.; Chung, W.Y.; Kwon, T.H.; Jayasankar, C.P.; Haritha, P. Venkatramu, V. Luminescence properties of Lu 3 Al 5 O 12: Tb 3+ nano-garnet. *J. Korean Phys. Soc*. **2014,** 64, 1859-1865.

[14] Oliveira, D.S.; Henrique, H.; Cebim, M. A.; da Silva, A. A.; Davolos, M. R. Structural and Spectroscopic Studies of Pr3+-Doped GdAlO3. *IEEE Trans. Nucl. Sci.***2010,** 57, 1260-1263.

[15] Cizauskaite, S.; Reichlová, V.; Nenartaviciene, G.; Beganskiene, A.; Pinkas, J.; Kareiva, A. Sol–gel preparation and characterization of gadolinium aluminate. *Mater. Chem. Phys.* **2007,** 102, 105-110.

[16] Girish, H. N.; Vijaya Kumar, M. S.; Byrappa, K.; Basavalingu, B. Hydrothermal synthesis of some of lanthanide aluminum perovskites–LnAlO3 (Ln= La, Sm and Gd). *Mater. Res. Innovations*. **2015,** 19, 270-274.

[17] Saji, S. K.; Vinodkumar, R.; Eappen, S. M.; Wariar, P. Optical and dielectric characterization of gadolinium aluminate ceramic nanoparticles synthesized by combustion technique. *Mater. Chem. Phys*.**2017,** 189-195.

[18] Dhananjaya, N.; Nagabhushana, H.; Nagabhushana B., M.; Chakradhar R., P., S.; Shivkumara, C.; Rudraswamy, C. Synthesis, characterization and photoluminescence properties of Gd2O3: Eu3+ nanophosphors prepared by solution combustion method, *Physica B: Condenser Matter*. **2010,** 17, 3795-3799.

[19] Dubnikova, N.; Garskaite, E.; Pinkas, J.; Bezdicka, P.; Beganskiene, A.; Kareiva, A. Sol–gel preparation of selected lanthanide aluminum garnets. *J. Sol-Gel Sci. Technol*. **2010,** 213-219.

[20] Tamrakar, R.K.; Bisen, D.B.; Nameeta Brahme, N. "Effect of Yb3+ concentration on photoluminescence properties of cubic Gd2O3 phosphor. *Infrared Physics & Technology*. **2015,** 92-97.

[21] Xia, G.; Zhou, S.; Zhang, J.; Wang, S.; Wang, H.; Xu, J. Sol–gel combustion synthesis and luminescence of Y4Al2O9: Eu3+ nanocrystal. *J. Non-Cryst. Solids.* **2005,** 37-39, 2979-2982.

[22] Zhang, Y.; Yu, H. Synthesis of YAG powders by the co-precipitation method. *Ceram. Int.* **2009,** 5, 2077-2081.

[23]https://www.researchgate.net/publication/375715426_infrared_and_raman_spectroscopy_study_of_y_3_al_5_o_12_nanoceramics_doped_50_Ho3, (2018).

[24] Guo, H.; Yin, M.; Dong, N.; Xu, M.; Lou, L.; Zhang, W. Effect of heat-treatment temperature on the luminescent properties of Lu2O3: Eu film prepared by Pechini sol–gel method. *Appl. Surf. Sci*. **2005**, 1-4, 245-250.

[25] Rekik, B.; Alombert-Goget, G.; Berthelot, A.; Benamara, O.; Lebbou, K. Optical properties of 2 at%(Ln3+) doped LiGd (WO4) 2 with Ln; Eu, Er and Tm, grown by μ-pulling down technique. *J. Alloys Compd.* **2020,** 154165.

[26] Som, S.; Sharma, S. K.; and Lochab, S. P. Swift heavy ion induced structural and optical properties of Y2O3: Eu3+ nanophosphor. *Mater. Res. Bull*. **2013,** 2, 844-851.

[27] Yamaguchi, O.; Takeoka, K.; Hirota, K.; Takano, H.; Hayashida, A. Formation of alkoxy-derived yttrium aluminum oxides. *J. Mater. Sci.***1992,** 1261-1264.

[28] Chen, Q.; Li, J. Wang, W. Synthesis and luminescence properties of Tb3+/Eu3+ co-doped GdAlO3 phosphors with enhanced red emission. *J. Rare Earths*. **2018,** 9, 924-930.

[29] Oliveira, H. H. S.; Cebim, M. A.; Da Silva, A. A.; Davolos, M. R. Structural and optical properties of GdAlO3: RE3+ (RE= Eu or Tb) prepared by the Pechini method for application as X-ray phosphors. *J. Alloys Compd*. **2009,** 2, 619-623.

[30] Muresan, L. E.; Popovici, E. J.; Perhaita, I.; Indrea, E.; Silipas, T. D. Effect of the europium doping on the structural and luminescent properties of yttrium aluminum garnet. *Mater. Sci. Eng*: B. **2013,** 4, 248-253.

[31] Boukerika, A.; Guerbous, L.; Chelef, H.; Benharrat, L. Preparation and characterization of bright high quality YAG: Eu^{3+} thin films grown by sol–gel dip-coating technique. *Thin solid films*. **2019,** 74-81.

[32] Vondrášková, A.; Beitlerova, A.; Barta, J.; Čuba, V.; Mihokova, E.; Nikl, M. Nanocrystalline Eu-doped Lu3Al5O12 phosphor prepared by radiation method. *Opt. Mater*. **2015,** 102-106.